

DEFECT ACCUMULATION IN RUBBER*

C. M. ROLAND AND C. R. SMITH†

THE FIRESTONE TIRE AND RUBBER COMPANY, CENTRAL RESEARCH LABORATORIES, 1200 FIRESTONE PARKWAY, AKRON, OHIO 44317

INTRODUCTION

The fracture of polymeric materials is accompanied, and to a large extent governed, by the generation of damaged material in the vicinity of a macroscopic crack¹⁻³. The observed crack propagation is, in general, not the direct result of the applied loading, but rather it represents the evolution of existing microcracks⁴. This microdamage can be the consequence of the same loading being used to drive the macrocrack or have arisen during specimen preparation. An understanding of the strength of materials requires consideration of both the nature of this defect accumulation as well as how the microcracks are transformed into macroscopic fracture planes by the applied stresses.

Although molecular theories of fracture have been developed^{5,6}, it is usually not feasible to directly connect the processes occurring at the molecular level to the macroscopic damage. In the case of a nonlinear, highly deformable, viscoelastic material such as rubber, an analysis of the stress field in the vicinity of a fracture plane and of the detailed structure of the material in this region is exceedingly difficult. For this reason, the tear and cut-growth behavior of rubber is usually treated through the use of a global energy criterion, wherein it is assumed that the complex phenomena occurring at the crack tip need not be considered explicitly since this region just translates without change at the same rate as the growing crack. The fracturing is then interpreted in terms of the elastically stored energy released per unit increase in crack area⁷. Various investigators have studied the stress field and hysteresis occurring in the fracture region^{8,9} and how the crack tip size and shape can affect the tear behavior of rubber^{10,11}. However, despite mention of such a phenomenon in rubber two decades ago¹², and the more recent elaboration of a thermodynamic analysis of the problem¹³, the question of how the material in the vicinity of the crack tip can accumulate damage, and moreover how this condition of the material can influence the observed tear behavior, has been largely ignored.

This article describes measurements of the damage in rubber samples existing in the region adjacent to a fracture plane as a result of the processes that gave rise to the fracture itself.

EXPERIMENTAL

The elastomers used in this work were Diene 35, a 90% 1,4-polybutadiene (BR), and FR-S1502, a 23.5% styrene emulsion SBR, both manufactured by the Firestone Tire and Rubber Company. Crosslinking of these materials was accomplished with α - α -bis(*t*-butylperoxy)diisopropylbenzene (Vulcur R of the

*Received January 30, 1985; revised April 29, 1985. B.

†Current address: Carnegie-Mellon University, Pittsburgh, Pennsylvania.

TABLE I
CROSSLINK DENSITY DATA ON SAMPLES AS DETERMINED FROM
STRESS-STRAIN MEASUREMENTS

Sample	SBR	BR
Stress, kPa	98	150
Extension ratio	1.156	1.156
ν , cm^{-3}	5.8×10^{19}	8.9×10^{19}
M_c , g/mole	10000	6800

Hercules Chemical Company). Vulcanization was carried out at 160°C for 20 min. The states of cure of the samples used are indicated in Table I, where the values for the effective crosslink density, ν , were obtained from the equilibrium stress, σ , at the extension ratio, $\lambda = 1.156$,

$$\nu = \left(\lambda - \frac{1}{\lambda^2} \right)^{-1} \frac{\sigma}{RT}, \quad (1)$$

where $T = 298^\circ\text{K}$ and R is the gas constant¹⁴. An Imass, Inc. Dynastat was used for the stress relaxation measurements. The 1.9 cm wide samples were fractured in tension using an Instron Universal Testing Instrument at a cross-head separation rate of 25.4 cm per min (which roughly corresponds to a 0.033 sec^{-1} deformation rate for the initial sample length employed). Only samples whose fracture surface was relatively smooth (*i.e.*, the scale of roughness did not exceed a few tenths of a millimeter) were actually used for the scattering measurements. In this manner, the x-ray beam would not be simultaneously both in and out of the specimen along the beam's length when measurements of scattering intensity were being made precisely at the fracture surface.

A Rigaku RU200 x-ray generator in combination with a Rigaku 2202 small angle scattering goniometer was used for the x-ray measurements. Data were

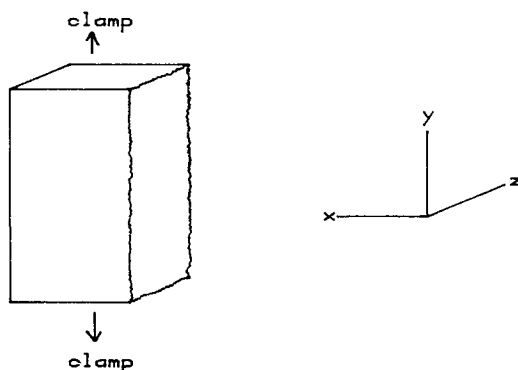


FIG. 1.—The incident x-ray beam propagated along the z-axis, perpendicular to the plane of the sample, with intensity measurements recorded in the xy plane. The sample could be translated along the x direction in order to determine how the scattering behavior of the material depended upon proximity to the fracture front.

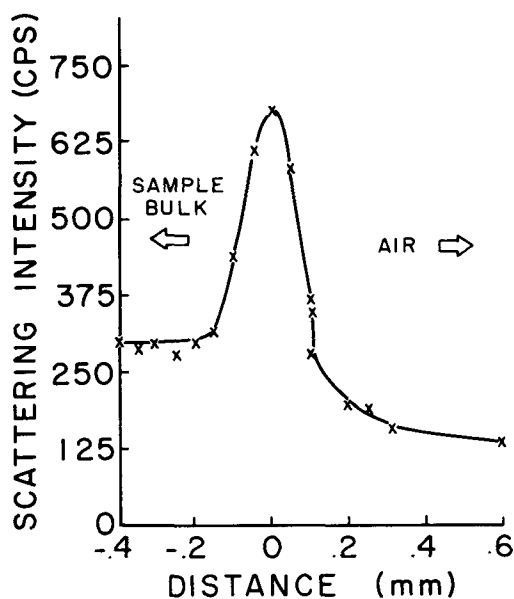


FIG. 2.—The SAXS intensity measured at $h = 0.009 \text{ \AA}^{-1}$ for the SBR sample as a function of the position in the sample relative to the crack front. Positive values of the abscissa indicate the beam is no longer passing through the sample.

collected at a scattering vector, h , down to 0.0046 \AA^{-1} ($1 \text{ \AA} = 0.1 \text{ nm}$) where

$$h = \frac{4\pi}{\lambda} \sin(\theta/2). \quad (2)$$

This corresponds to a scattering angle, θ , equal to 0.065° for Cu K_α radiation ($\lambda = 1.54 \text{ \AA}$).

The x-ray samples were mounted in a clamp attached to a translator with a micrometer drive. Slit collimation was employed with the x-ray beam parallel to the crack surface (Figure 1). The scattered intensity could in this manner be taken as a function of position in the sample relative to the fracture surface.

RESULTS AND DISCUSSION

Displayed in Figure 2 is the small-angle x-ray intensity measured at $h = 0.009 \text{ \AA}^{-1}$ as a function of the position of the incident beam relative to the crack surface in the SBR sample. Away from this crack edge, there occurs scattering from within the sample bulk as a consequence of thermal fluctuations in the electron density of the sample¹⁵ (which is a homogeneous, amorphous material). When the incident beam does not pass through the sample, a weak background intensity can be measured which is due primarily to diffuse scattering from the collimation system. At precisely the crack edge, it can be observed in Figure 2 that the scattering intensity increases markedly. This scattering is due to microcracks existing in the vicinity of the fracture plane. The breadth of the peak in Figure 2 corresponds to the roughness of the torn surface (about 200 \mu m);

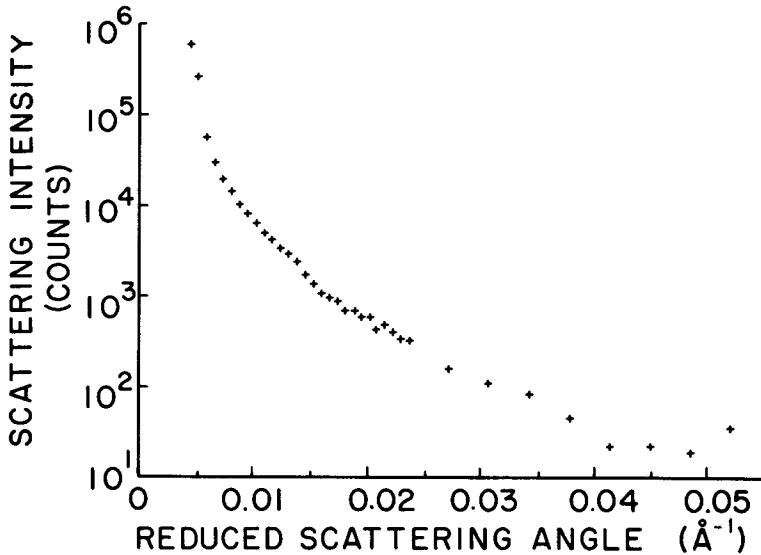


FIG. 3.—SAXS curve measured for the SBR sample with the primary beam incident at the crack edge. Background scattering from the sample bulk has been subtracted.

consequently, it can be inferred only that the width of the damaged zone around the crack is not larger than this 200 μm .

After subtraction of the scattering originating from within the sample bulk, the small-angle x-ray scattering (SAXS) intensity measured as a function of the angle of scattering is displayed in Figure 3. In principle, the size distribution of the scattering entities, in this case microvoids, can be extracted from the angle dependence of the scattering. An often employed analysis is that of Guinier¹⁶, where use is made of the fact that for an isotropic system exhibiting no long range order, the scattering function can be expanded in a series whose first two terms are identical with the first two terms in the series expansion of an exponential function. Accordingly, for small h , the scattering intensity is approximated by

$$I(h) = I(0) \exp(-R^2 h^2/3). \quad (3)$$

The data of Figure 3 when plotted in the form $\ln I(h)$ versus h^2 (the well known Guinier plot) is not linear. This indicates that at the smallest h accessible in these experiments, 0.0046\AA^{-1} , the two-term truncation referred to above is not valid. The reason for this is that the radius of gyration, R , of the microcracks exceeds the inverse of this minimum value of h ; *i.e.*,

$$\begin{aligned} R &> (0.0046)^{-1} \\ &> 220 \text{\AA} \end{aligned}$$

Damage evolution is a statistical process, so that the microscopic cracks are likely to exist over a wide range of sizes. The nonlinearity of the Guinier plots in this case would be due to the size distribution extending beyond 200 \AA .

An alternative approach to interpretation of scattering data is through the use of integral parameters¹⁷. A correlation length, l_c , and volume, v_c of the particles can be obtained through integration of functions of the scattered intensities,

$$l_c = \frac{\pi \int_0^\infty hI(h)dh}{\int_0^\infty h^2I(h)dh}, \quad (4)$$

$$v_c = \frac{2\pi^2I(0)}{\int_0^\infty h^2I(h)dh}. \quad (5)$$

The required extrapolation to zero angle can be accomplished with reasonable accuracy only when an approximation such as Equation (3) can be made. An accurate estimation of these integral parameters can, on the other hand, be made if the extrapolated area contributes only a small part to the integration. This is not the case in the present situation, where the scattered intensity, even when multiplied by the scattering angle, is still increasing as one proceeds down to the smallest h at which measurements could be made. Once again, the difficulty originates from the large size of the microcracks. While heterogeneities in electron density extending over as much as 1000 Å will give rise to SAXS, the extraction from the data of size estimations is generally not possible when the particles (or voids) exceed a few hundred Angstroms, or exist over a range of sizes extending beyond this magnitude.

Although with the present instrumental arrangement it is not possible to obtain information concerning the size of the microcracks, other aspects of their formation in rubber could be investigated. Of particular interest is the relationship between a sample's brittleness and the generation of this microdamage. An SBR specimen was prepared with a crosslink density about 33% less than that of the sample for which the data shown above were obtained. It was fractured in a similar fashion and examined in the small-angle x-ray instrument. No enhanced scattering in the vicinity of the crack front could be detected. Evidently, in a more compliant sample, flow processes are dominant in the highly stressed region at the crack front, so that there is a negligible extent of microcracking. Contrarily, a highly crosslinked BR specimen (see Table I) showed very intense scattering in the vicinity of the fracture surface, as is seen in Figure 4. While a quantitative comparison of the data in Figure 2 and Figure 4 must be made with caution in view of the differences in experimental conditions (*e.g.*, the data for the BR sample were obtained at $h = 0.006 \text{ \AA}^{-1}$), it is obvious that from the more brittle sample, there is significantly more x-ray scattering. It is, of course, well known that the fracture of plastics is accompanied by extensive microscopic crack formation¹. The absence of previous recognition of the phenomenon in rubbers may be due to the sensitivity of this damage evolution to the level of crosslinking in rubbers.

It was interesting to find that the observation of the microcracks did not require any elongation of the sample; that is, it was not necessary to "open up" the microcracks in order to detect them. This indicates that upon fracture the surfaces do not completely rejoin after removal of the load. Similar effects are well known in plastics and metals. In fact, if the SBR specimen is elongated during the SAXS measurement, the scattering intensity becomes time-dependent

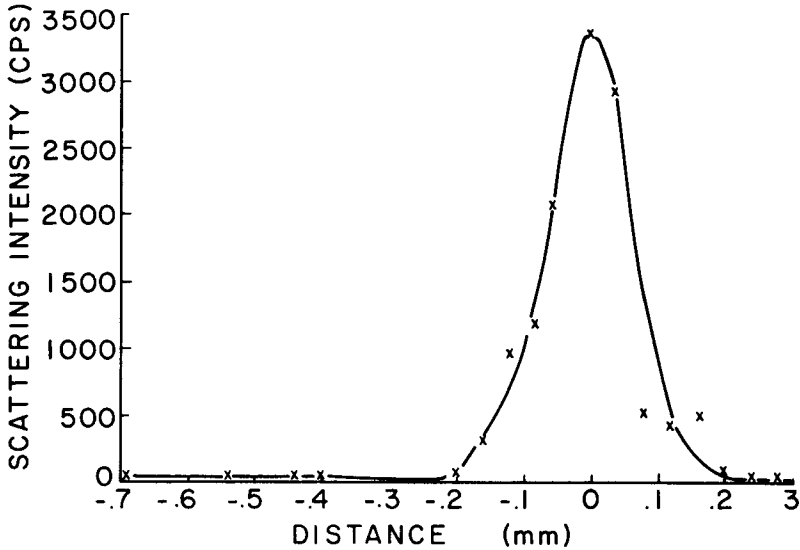


FIG. 4.—The scattering intensity measured at $h = 0.006 \text{ \AA}^{-1}$ for the BR sample as a function of the position of the incident beam relative to the crack edge.

(Figure 5). The damage accumulation process continues as the sample is held at a fixed strain. For comparison purposes, the stress relaxation behavior of this sample at 15.6% elongation is displayed in Figure 6. It must be realized from data such as this that the hysteresis and stress relaxation behavior observed in elastomers is at least in part due to the creation of new surface area, particularly when the sample is brittle. Although it obviously depends upon the strain

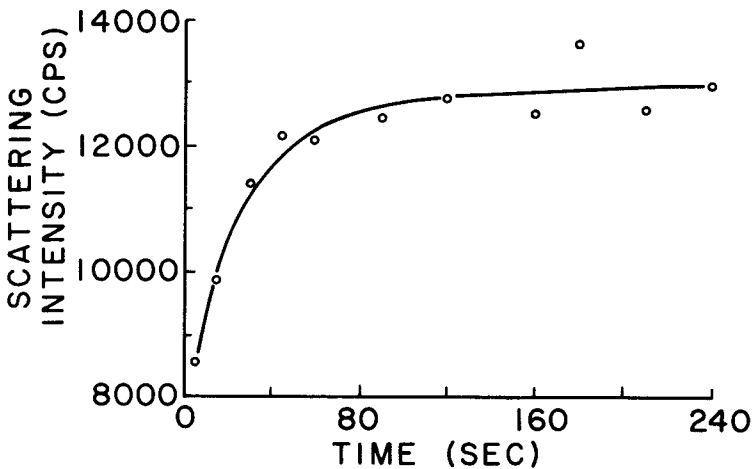


FIG. 5.—The SAXS intensity measured from the SBR sample as a function of the time at which it had been held at a tensile elongation of 35%. The scattering angle was maintained at 0.007 \AA^{-1} .

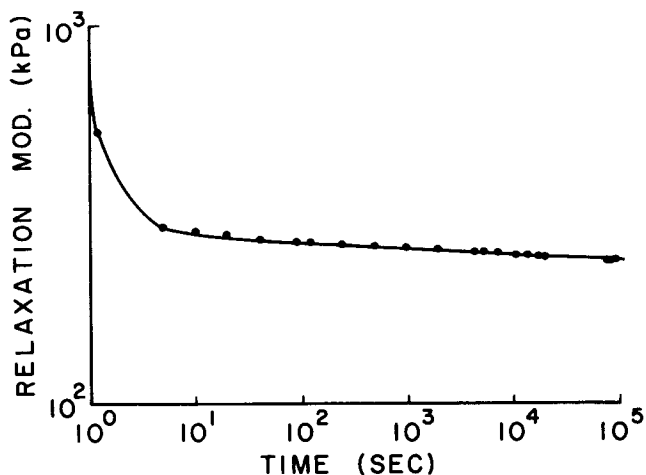


FIG. 6.—Stress relaxation behavior of the SBR sample at room temperature at $\lambda = 1.156$.

imposed upon the sample, it has been determined, for example, that in fiberglass, the energy due to creation of microscopic fracture surfaces accounts for 20 to 30% of the mechanical hysteresis¹. While the value is expected to be less in rubber samples, its role in the tear behavior of the elastomers remains to be investigated. If one unloads the SBR sample, the SAXS measurements are not reversible (Figure 7). This is due both to the influence of the shape of the microcracks on the scattering intensity (this shape changing with strain), as well as to the kinetics of the damage and healing processes simultaneously occurring.

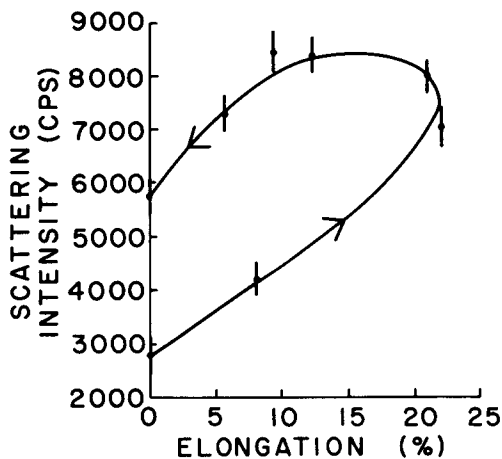


FIG. 7.—The change in SAXS intensity as the SBR sample is elongated and then retracted. The measurements were taken at $h = 0.007 \text{ \AA}^{-1}$. To allow for the Poisson contraction of the rubber, the primary beam position was adjusted to maintain its location constant relative to the crack front.

It was observed that fractured samples, for which initially there occurred intense scattering from the vicinity of the crack surface, would after a week exhibit a much reduced level of scattering. While no quantitative measurements of this effect were attempted, it is evident that a healing process is operative. The original material strength can not, of course, be regained, since covalent bonds have been broken during fracture; however, entanglement of chain ends serves to close the microcracks sufficiently to diminish the x-ray scattering.

SUMMARY

It has been demonstrated that the material adjacent to the fracture plane in cured rubber specimens can scatter intense x-ray radiation at small angles. This phenomenon is associated with the presence in the material of voids of very small size. These microvoids exist only adjacent to the fracture surface and are the result of the loading imposed to create the macroscopic fracture. The significance of these microscopic defects is their influence on the manner in which externally applied loads produce fracture of rubber; that is, they provide a link between the experimentally observed fracture behavior of rubbers and the fundamental processes governing this behavior. To cite a few examples, it has been observed that the critical value of tearing energy required for catastrophic failure of a rubber specimen differs for a static *versus* dynamic mode of deformation¹⁸. It can be recognized that these differences are related, not only to rate effects, but also to the differences in the state of the fractured material directly in front of the crack tip. It has also been noted that the manner in which one introduces a precut into a rubber test specimen can influence the ensuing strength measurement by affecting the nature of the initial fracture plane¹⁹. It should be understood that the test result can be affected not only by such differences in the geometry of the precut, but as well by the effect the precutting can have on the condition of the unfractured material adjacent to the precut.

Currently, our efforts are being directed towards modification of the SAXS instrument to permit measurements to be made at lower values of scattering angle. It is hoped that this will allow quantification of the size and abundance of the microcracks. Such information can provide insight into the significance of defect accumulation in the development of tear resistance in elastomers.

ACKNOWLEDGMENTS

The authors would like to thank Dr. G. G. A. Böhm for his support and encouragement during the course of this work and the Firestone Tire and Rubber Company for permission to publish this paper.

REFERENCES

- ¹ V. S. Kuksenko and V. P. Tamuzs, "Fracture MicroMechanics, of Polymer Materials," Martinus Nijhoff, The Hague, 1981.
- ² N. J. Wells and N. Walker, *J. Mater. Sci.* **15**, 1832 (1980).
- ³ W. G. Knauss, Ph.D. Thesis, California Institute of Technology, Pasadena, CA, June 1963.
- ⁴ A. Chudnovsky and A. Moet, *Polym. Eng. Sci.* **22**, 22 (1982).
- ⁵ F. Bueche and J. C. Halpin, *J. Appl. Phys.* **35**, 36 (1964); J. C. Halpin, *RUBBER CHEM. TECHNOL.* **38**, 1007 (1965).
- ⁶ V. R. Regel, A. I. Slutsker, and E. E. Tomashevskii, *Sov. Phys. Usp.* **15**, 45 (1972).
- ⁷ R. S. Rivlin and A. G. Thomas, *J. Polym. Sci.* **10**, 291 (1953).
- ⁸ W. G. Knauss, *Exp. Mech.* **8**, 177 (1968).

- ⁹ E. H. Andrews, *J. Mech. Phys. Solids* **11**, 231 (1963).
- ¹⁰ H. W. Greensmith, L. Mullins, and A. G. Thomas, *Trans. Soc. Rheol.* **4**, 179 (1960).
- ¹¹ A. Kadir and A. G. Thomas, *RUBBER CHEM. TECHNOL.* **54**, 15 (1981).
- ¹² L. Mullins, *Trans. Inst. Rubber Ind.* **35**, 213 (1959).
- ¹³ A. Chudnovsky, I. Palley, and E. Baer, *J. Mater. Sci.* **16**, 35 (1981).
- ¹⁴ P. J. Flory, "Principles of Polymer Chemistry," Cornell University Press, Ithaca, N.Y., 1953.
- ¹⁵ W. Wiegand and W. Ruland, *Prog. Colloid Polym. Sci.* **66**, 355 (1979).
- ¹⁶ A. Guinier and G. Fournet, "Small Angle Scattering of X-rays," Wiley, New York, 1955.
- ¹⁷ G. Porod in "Small-Angle X-ray Scattering," H. Brumberger, Ed., Gordon and Breach, New York, 1967.
- ¹⁸ P. B. Lindley, *Int. J. of Fract.* **9**, 449 (1973).
- ¹⁹ A. G. Thomas, *J. Polym. Sci.* **31**, 467 (1958).